Film-free laser forward printing of transparent and weakly absorbing liquids

M. Duocastella, A. Patrascioiu, J. M. Fernández-Pradas, J. L. Morenza, and P. Serra*

Universitat de Barcelona, Departament de Física Aplicada i Òptica, Martí i Franquès 1, 08028-Barcelona, Spain
**pserra@ub.edu*

Abstract: A laser-based technique for printing transparent and weakly absorbing liquids is developed. Its principle of operation relies in the tight focusing of short laser pulses inside the liquid and close to its free surface, in such a way that the laser radiation is absorbed in a tiny volume around the beam waist, with practically no absorption in any other location along the beam path. If the absorbed energy overcomes the optical breakdown threshold, a cavitation bubble is generated, and its expansion results in the propulsion of a small fraction of liquid which can be collected on a substrate, leading to the printing of a microdroplet for each laser pulse. The technique does not require the preparation of the liquid in thin film form, and its forward mode of operation imposes no restriction concerning the optical properties of the substrate. These characteristics make it well suited for printing a wide variety of materials of interest in diverse applications. We demonstrate that the film-free laser forward printing technique is capable of printing microdroplets with good resolution, reproducibility and control, and analyze the influence of the main process parameter, laser pulse energy. The mechanisms of liquid printing are also investigated: time-resolved imaging provides a clear picture of the dynamics of liquid transfer which allows understanding the main features observed in the printed droplets.

OCIS codes: (310.1860) Deposition and fabrication; (350.3390) Laser materials processing; (140.3440) Laser-induced breakdown; (140.7090) Ultrafast lasers; (110.6915) Time imaging.

References

1. M. L. Levene, R. D. Scott, and B. W. Siryj, "Material transfer recording," Appl. Opt. **9**(10), 2260–2265 (1970).
2. J. Bohandy, B. F. Kim, and F. J. Adrian, "Metal-deposition from a supported metal-film using an excimer laser," J. Appl. Phys. **60**(4), 1538–1539 (1986).
3. I. Zergioti, S. Mailis, N. A. Vainos, P. Papakonstantinou, C. Kalpouzos, C. P. Grigoropoulos, and C. Fotakis, "Microdeposition of metal and oxide structures using ultrashort laser pulses," Appl. Phys., A Mater. Sci. Process. **66**(5), 579–582 (1998).
4. A. Piqué, D. B. Chrisey, R. C. Y. Auyeung, J. Fitz-Gerald, H. D. Wu, R. A. McGill, S. Lakeou, P. K. Wu, V. Nguyen, and M. Duignan, "A novel laser transfer process for direct writing of electronic and sensor materials," Appl. Phys., A Mater. Sci. Process. **69**(7), S279–S284 (1999).
5. A. Piqué, D. B. Chrisey, J. M. Fitz-Gerald, R. A. McGill, R. C. Y. Auyeung, H. D. Wu, S. Lakeou, V. Nguyen, R. Chung, and M. Duignan, "Direct writing of electronic and sensor materials using a laser transfer technique," J. Mater. Res. **15**(9), 1872–1875 (2000).
6. C. B. Arnold, P. Serra, and A. Piqué, "Laser direct-write techniques for printing of complex materials," MRS Bull. **32**, 23–31 (2007).
7. L. Rapp, A.K. Diallo, A.P. Alloncle, C. Videlot-Ackermann, F. Fages and P. Delaporte, "Pulsed-laser printing of organic thin-film transistors," Appl. Phys. Lett. **95**, 171109 (2009).
8. H. Kim, R. C. Y. Auyeung, S. H. Lee, A. L. Huston, and A. Pique, "Laser forward transfer of silver electrodes for organic thin-film transistors," Appl. Phys., A Mater. Sci. Process. **96**(2), 441–445 (2009).
9. C. Boutopoulos, V. Tsouti, D. Goustouridis, S. Chatzandroulis and I. Zergioti, "Liquid phase direct laser printing of polymers for chemical sensing applications," Appl. Phys. Lett. **93**, 191109 (2008).
10. M. Colina, P. Serra, J. M. Fernández-Pradas, L. Sevilla, and J. L. Morenza, "DNA deposition through laser induced forward transfer," Biosens. Bioelectron. **20**(8), 1638–1642 (2005).
11. I. Zergioti, A. Karaiskou, D.G. Papazoglou, C. Fotakis, M. Kapsetaki and D. Kafetzopoulos, "Femtosecond laser microprinting of biomaterials," Appl. Phys. Lett. **86**, 163902 (2005).

#132085 - $15.00 USD Received 22 Jul 2010; revised 10 Sep 2010; accepted 10 Sep 2010; published 29 Sep 2010

12. V. Dinca, M. Farsari, D. Kafetzopoulos, A. Popescu, M. Dinescu, and C. Fotakis, "Patterning parameters for biomolecules microarrays constructed with nanosecond and femtosecond UV lasers," Thin Solid Films **516**(18), 6504–6511 (2008).
13. M. Duocastella, J. M. Fernández-Pradas, J. Domínguez, P. Serra, and J. L. Morenza, "Printing biological solutions through laser-induced forward transfer," Appl. Phys., A Mater. Sci. Process. **93**(4), 941–945 (2008).
14. B. Hopp, T. Smausz, N. Kresz, N. Barna, Z. Bor, L. Kolozsvári, D. B. Chrisey, A. Szabó, and A. Nógrádi, "Survival and proliferative ability of various living cell types after laser-induced forward transfer," Tissue Eng. **11**(11-12), 1817–1823 (2005).
15. A. Doraiswamy, R. Narayan, T. Lippert, L. Urech, A. Wokaun, M. Nagel, B. Hopp, M. Dinescu, R. Modi, and R. Auyeung, "Excimer laser forward transfer of mammalian cells using a novel triazene absorbing layer," Appl. Surf. Sci. **252**(13), 4743–4747 (2006).
16. B. R. Ringeisen, C. M. Othon, J. A. Barron, D. Young, and B. J. Spargo, "Jet-based methods to print living cells," Biotechnol. J. **1**(9), 930–948 (2006).
17. M. Colina, M. Duocastella, J.M. Fernández-Pradas, P. Serra and J.L. Morenza, "Laser-induced forward transfer of liquids: study of the droplet ejection process," J. Appl. Phys. **99**, 084909 (2006).
18. N.T. Kattamis, P.E. Purnick, R. Weiss and C.B. Arnold, "Thick film laser induced forward transfer for deposition of thermally and mechanically sensitive materials," Appl. Phys. Lett. **91**, 171120 (2007).
19. N.T. Kattamis, N.D. McDaniel, S. Bernhard and C.B. Arnold, "Laser direct write printing of sensitive and robust light emitting organic molecules," Appl. Phys. Lett. **94**, 103306 (2009).
20. M. Duocastella, J. M. Fernández-Pradas, J. L. Morenza, D. Zafra, and P. Serra, ""Novel laser printing technique for miniaturized biosensors preparation," Sens. Act," Biol. Chem. **145**, 596–600 (2010).
21. A. Vogel, S. Busch, and U. Parlitz, "Shock wave emission and cavitation bubble generation by picosecond and nanosecond optical breakdown in water," J. Acoust. Soc. Am. **100**(1), 148–165 (1996).
22. C. B. Schaffer, N. Nishimura, E. N. Glezer, A. M. T. Kim, and E. Mazur, "Dynamics of femtosecond laser-induced breakdown in water from femtoseconds to microseconds," Opt. Express **10**(3), 196–203 (2002).
23. C. B. Schaffer, A. Brodeur, and E. Mazur, "Laser-induced breakdown and damage in bulk transparent materials induced by tightly focused femtosecond laser pulses," Meas. Sci. Technol. **12**(11), 1784–1794 (2001).
24. C. L. Arnold, A. Heisterkamp, W. Ertmer, and H. Lubatschowski, "Computational model for nonlinear plasma formation in high NA micromachining of transparent materials and biological cells," Opt. Express **15**(16), 10303–10317 (2007).
25. P. G. de Gennes, "Wetting - statics and dynamics," Rev. Mod. Phys. **57**(3), 827–863 (1985).
26. J. A. Barron, H. D. Young, D. D. Dlott, M. M. Darfler, D. B. Krizman, and B. R. Ringeisen, "Printing of protein microarrays via a capillary-free fluid jetting mechanism," Proteomics **5**(16), 4138–4144 (2005).
27. P. Serra, M. Colina, J. M. Fernández-Pradas, L. Sevilla, and J. L. Morenza, "Preparation of functional DNA microarrays through laser-induced forward transfer," Appl. Phys. Lett. **85**(9), 1639–1641 (2004).
28. Y. Lin, Y. Huang and D.B. Chrisey, "Droplet formation in matrix-assisted pulsed-laser evaporation direct writing of glycerol-water solution," J. Appl. Phys. **105**, 093111 (2009).
29. E. N. Glezer, C. B. Schaffer, N. Nishimura, and E. Mazur, "Minimally disruptive laser-induced breakdown in water," Opt. Lett. **22**(23), 1817–1819 (1997).
30. A. Vogel, N. Linz, S. Freidank and G. Paltauf, "Femtosecond-laser-induced nanocavitation in water: implications for optical breakdown threshold and cell surgery," Phys. Rev. Lett. **100**, 038102 (2008).
31. J. R. Blake, and D. C. Gibson, "Growth and collapse of a vapor cavity near a free-surface," J. Fluid Mech. **111**(-1), 123–140 (1981).
32. A. Pearson, E. Cox, J. R. Blake, and S. R. Otto, "Bubble interactions near a free surface," Eng. Anal. Bound. Elem. **28**(4), 295–313 (2004).
33. M. Duocastella, J. M. Fernández-Pradas, P. Serra, and J. L. Morenza, "Jet formation in the laser forward transfer of liquids," Appl. Phys., A Mater. Sci. Process. **93**(2), 453–456 (2008).
34. M. Duocastella, J.M. Fernández-Pradas, J.L. Morenza and P. Serra, "Time-resolved imaging of the laser forward transfer of liquids," J. Appl. Phys. **106**, 084907 (2009).
35. J. Eggers, "Nonlinear dynamics and breakup of free-surface flows," Rev. Mod. Phys. **69**(3), 865–930 (1997).
36. B. W. Zeff, B. Kleber, J. Fineberg, and D. P. Lathrop, "Singularity dynamics in curvature collapse and jet eruption on a fluid surface," Nature **403**(6768), 401–404 (2000).
37. L. Duchemin, S. Popinet, C. Josserand, and S. Zaleski, "Jet formation in bubbles bursting at a free surface," Phys. Fluids **14**(9), 3000–3008 (2002).
38. A. M. Worthington, and R. S. Cole, "Impact with a liquid surface studied by the aid of instantaneous photography," Philos. Trans. R. Soc. Lond. A **25**, 261–498 (1897).
39. M. Rein, "Phenomena of liquid-drop impact on solid and liquid surfaces," Fluid Dyn. Res. **12**(2), 61–93 (1993).
40. J. Shin, and T. A. Mcmahon, "The tuning of a splash," Phys. Fluids A **2**(8), 1312–1317 (1990).
41. A. Ogawa, K. Utsuno, M. Mutou, S. Kouzen, Y. Shimotake, and Y. Satou, "Morphological study of cavity and Worthington jet formations for newtonian and non-newtonian liquids," Particul. Sci. Technol. **24**(2), 181–225 (2006).
42. M. Duocastella, J. M. Fernández-Pradas, J. L. Morenza, and P. Serra, "Sessile droplet formation in the laser-induced forward transfer of liquids: a time-resolved imaging study," Thin Solid Films **518**(18), 5321–5325 (2010).

#132085 - $15.00 USD Received 22 Jul 2010; revised 10 Sep 2010; accepted 10 Sep 2010; published 29 Sep 2010

1. Introduction

The most extended laser direct write technique allowing the deposition of materials with high resolution is laser-induced forward transfer (LIFT). In LIFT, a pulsed laser is used to produce the transfer of material from a donor thin film onto a receptor substrate placed facing the film and usually at a short separation from it. The laser pulse is focused on the donor film through its substrate (transparent to the laser radiation), and is absorbed there, generating the burst necessary to propel a small fraction of the film towards the receptor substrate, where that fraction is deposited. Translation of both donor and receptor substrates allows the generation of two-dimensional patterns. LIFT was initially conceived to operate with solid donor films [1,2] for the deposition of simple inorganic materials, mainly for microelectronic applications [2–4]. However, the extension of the concept to liquid films [5] converted LIFT in a true printing technique, and thus practically eliminated any restriction concerning the materials which could be deposited with it [6]. In this approach, the material of interest is dissolved or suspended in a liquid, and submitted to LIFT, leading to the deposition of the solution/suspension in the form of microdroplets. A great variety of complex materials has been successfully printed through LIFT: nanoparticle inks for electrodes in transistors [7,8], polymers for chemical sensors [9], biomolecule solutions for biosensors [10–13], or even living cells for tissue engineering applications [14–16].

Many materials of interest, like organic chemodetectors and semiconductors, biomolecules, cells or nanoparticles, are provided in solutions transparent to or weakly absorbing of the radiation of most lasers commonly used in microfabrication applications. This problem has been typically solved in LIFT through the intercalation of an absorbing solid layer between the transparent donor substrate and the liquid film. In this scheme, the laser radiation is absorbed in the intermediate layer, which is either ablated [9–17], or deformed [18,19] by the action of the laser pulse, thus providing the required thrust to propel some liquid away from the donor substrate. Most of the work devoted to the LIFT of liquids has been carried out through the use of absorbing layers.

The LIFT of liquids faces, however, an intrinsic drawback which compromises its future industrial implementation: the preparation of the liquid to be transferred in thin film form. Spreading uniform and stable liquid films is not easy, especially if areas larger than a few mm^2 are required, and the problem becomes really critical when, in addition, high resolutions are desired. In consequence, it would be convenient to have a laser printing technique with all the advantages of LIFT, but without the constraint of the liquid film preparation.

In this work the development of a new laser forward printing technique is presented. The technique allows printing transparent and weakly absorbing liquids without the need for the preparation of the liquid in thin film form. Although a similar objective was previously achieved with another film-free technique [20], its backward mode of printing limited its application to the use of transparent substrates. This represented a significant restriction which prevented printing on many technologically relevant substrates, like silicon wafers, metallic electrodes, or any patterned (though transparent) surface, for instance, lab-on-a-chip devices. The feasibility of the new technique is tested through microdroplets printing, and a study of the influence on their morphology of the main process parameter, laser pulse energy, is carried out. The study is not limited to the analysis of the performance of laser printing, but a deeper understanding of the process is pursued. To this end, liquid ejection is analyzed through time-resolved imaging, a characterization technique which should help determine the mechanisms responsible for microdroplets deposition. The obtained results reveal that printing proceeds through complex dynamics from which help explain the main features observed in the deposits.

2. Principle of operation

The principle of operation of the film-free laser forward printing technique relies on the generation of a cavitation bubble underneath the free surface of the liquid to be printed. Cavitation can be induced at any depth inside a transparent or weakly absorbing liquid by

#132085 - $15.00 USD Received 22 Jul 2010; revised 10 Sep 2010; accepted 10 Sep 2010; published 29 Sep 2010

tightly focusing a laser pulse at that depth. In these conditions, radiation absorption (which increases with intensity) would achieve its maximum in the laser beam waist. If such absorption is high enough to overcome the optical breakdown threshold of the liquid, a plasma can be generated, which would induce the formation of the cavitation bubble [21,22].

The focusing of a laser beam into an absorbing medium is sketched in a simplified way in Fig. 1a. It is assumed in the scheme that the laser beam is a plane wave of intensity I_o that is transformed by the focusing optics into a spherical wave which intensity is $I(z)$ at a focusing depth of z. The corresponding absorbed power per unit volume is given by $\alpha \cdot I(z)$ for an absorption coefficient α, and its evolution in depth is represented in the plot of Fig. 1b, where an arbitrary threshold for breakdown has been set.

Under linear absorption conditions α is constant (solid line in Fig. 1b), and according to the presented scheme breakdown would take place at a depth z_{B0}, making possible the generation of the cavitation bubble in that position, and therefore accomplishing the desired objective. However, it can be observed that in this case there would be significant absorption of radiation at depths well below z_{B0}, which would lead to the unnecessary and detrimental heating of a large portion of the medium along the laser beam path.

The previous scenario can be greatly enhanced under nonlinear absorption. In these conditions α is no longer constant, and its dependence with the intensity I is determined by the particular absorption mechanism taking place. Although several instances of nonlinear absorption could be considered, multiphoton absorption appears to be especially adequate thanks to its deterministic character [23]. In this case α would be proportional to I^k, being $k + 1$ the number of photons involved in the energetic transition associated with the absorption event. The dashed line in the plot of Fig. 1b corresponds to such instance. The sharper increase of $\alpha \cdot I$ respect to that of the linear case clearly reveals how much the localized character of absorption can be enhanced. Thus, the generation of the cavitation bubble in a position close to the beam waist is possible with practically no heating of the fraction of medium traversed by the beam path, a requisite that must be fulfilled in any application involving fragile materials. In order to achieve multiphoton absorption in most transparent and weakly absorbing liquids, the use of sub-picosecond laser pulses is required in addition to the tight focusing of the laser beam [23].

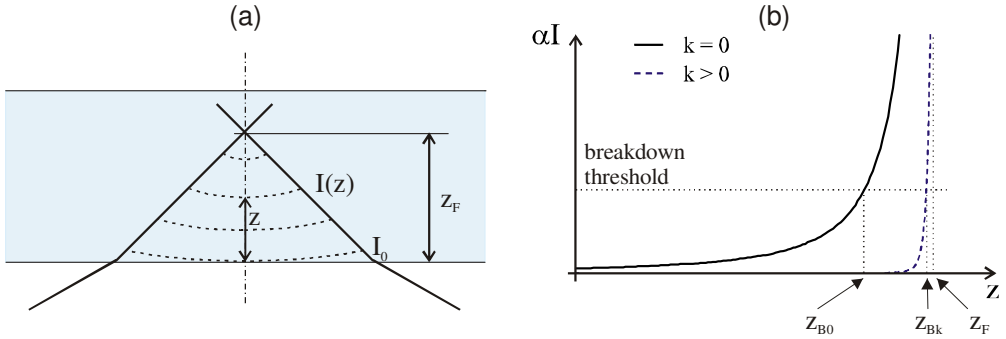

Fig. 1. a) Focusing of a plane wave of intensity I_o at a depth z_F inside a medium. The dashed curve at depth z represents a spherical front with intensity $I(z)$. b) Plot of the corresponding power absorbed per unit volume (αI) versus depth (z) for the case of linear (k = 0) and non-linear absorption (k>0). The dashed straight line indicates the optical breakdown threshold for the medium.

Although the attainment of optical breakdown through tightly focusing very short laser pulses is a far more complex situation than that described in the preceding paragraphs [24], the previous description contains the essential elements for understanding the method of production of a cavitation bubble inside the liquid. In consequence, and in spite of its simplicity, it serves well the purpose of illustrating the principle of operation of the laser forward printing technique.

#132085 - $15.00 USD Received 22 Jul 2010; revised 10 Sep 2010; accepted 10 Sep 2010; published 29 Sep 2010

Once generated, the cavitation bubble expands, displacing the liquid around it. If the bubble is produced close to the free surface, a fraction of the liquid could be propelled away, and collected onto a substrate. Provided that both the depth of the bubble and its pressure are the adequate ones, it can be expected that the liquid will be deposited on the substrate in the form of a well-defined droplet. For this to occur, both the laser pulse energy and focusing depth should be properly adjusted in order to allow liquid transfer devoid of splashing. According to this, the means for obtaining droplets of micrometric dimensions relies in focusing the laser beam in a very shallow position inside the liquid.

The proposed configuration which should make possible printing microdroplets of transparent or weakly absorbing liquids following the previously described principle of operation is schematized in Fig. 2. In addition to microdroplets printing, this configuration fulfills the prior stated conditions: it does not require the preparation of the liquid in thin-film form, and imposes no restrictions concerning the optical properties of the substrate. In this technique, each droplet results from a single laser pulse, and the generation of micropatterns can be achieved through the translation of the substrate respect to the laser beam.

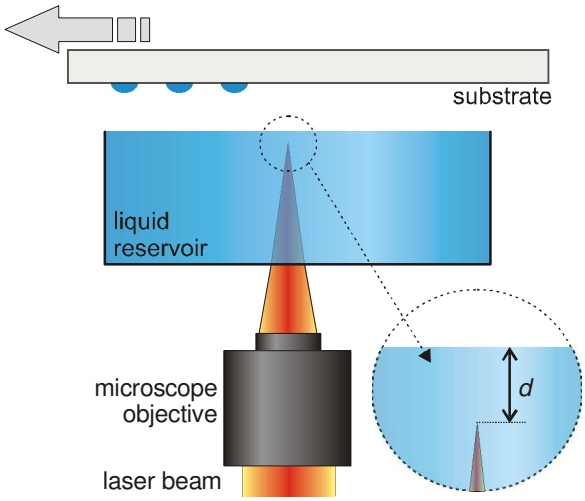

Fig. 2. Scheme of the film-free laser forward printing setup.

3. Experimental setup

The laser system used for this experiments was a diode pumped Yb:KYW femtosecond laser (1027 nm wavelength, 450 fs pulse duration, 1 kHz maximum repetition rate). The laser beam was focused inside the liquid to be deposited using a microscope objective (50 × , NA 0.55) with a working distance of 13 mm. The diameter of the laser beam waist in the focus was about 1.2 µm.

The liquid solution was a mixture of water and glycerol at 20% (v/v), kept in a reservoir consisting of a plastic container with a capacity of 1 mL. The reservoir was held on a z stage which allowed varying the position of the focal volume with respect to the liquid free-surface. The substrates were commercially available poly-L-lysine coated microscope slides, held on computer-controlled xyz translation stages which were synchronized with the laser pulses. The translation of the substrates along the x and y directions, while keeping the reservoir stationary, allowed the preparation of micropatterns. The distance between the liquid surface and the substrates in all the experiments was about 500 µm. The morphology of the deposited droplets was characterized by means of optical microscopy.

Time-resolved side view images of the liquid ejection process were acquired using an imaging system composed of an illuminating source (a cw Nd:YAG laser, 532 nm wavelength, 20 mW power), a divergent lens (1 m focal length) to provide a rather uniform illumination of the imaged region, a magnification system (a 15 × microscope objective with a

#132085 - $15.00 USD Received 22 Jul 2010; revised 10 Sep 2010; accepted 10 Sep 2010; published 29 Sep 2010

NA of 0.32 plus a teleobjective with a focal length of 100 mm), and finally a gated charged-coupled device (CCD) camera. The CCD had a resolution of 288 × 385 pixels, with 8 bits dynamic range, and it was intensified by a microchannel plate (MCP). The aperture of the MCP was synchronized with laser firing through a pulse generator. A single image frame was taken for each laser pulse, with an integration time of 100 ns, and varying the time delay between the laser pulse and the MCP aperture allowed reconstructing a stop-action movie of the transfer process.

4. Results

The feasibility of the laser forward printing technique was tested through the preparation of arrays of microdroplets. Figure 3 displays one of these microarrays, obtained at a focusing depth of about 20 µm below the liquid free surface, and at a laser pulse energy of around 4 µJ. The printed features indeed take the form of microdroplets, all well aligned, and with good uniformity in both shape and size. Most of them are circular, and only a very few present slight elongations in one of their sides, which suggest that the droplets suffered spreading during deposition and further shrinking; the elongations could correspond to pinning of a portion of the droplet receding contact line due to small defects in the substrate surface [25].

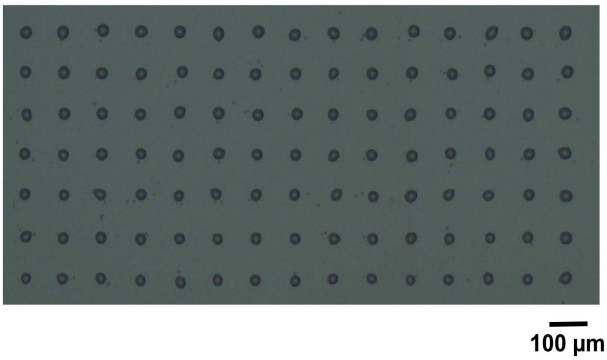

Fig. 3. Array of microdroplets printed with the film-free laser forward printing technique. The focusing depth is about 20 µm and the laser pulse energy is around 4.0 µJ. The droplets have a diameter of about 25 µm.

Such pinning could also account for the existence of the very small isolated satellite found in the vicinity of a few droplets. The droplets present a diameter of about 25 µm, a value which lies well below those routinely achieved with more conventional printing techniques [26], and not easy to attain with good uniformity in large arrays with traditional LIFT [27]. Obtaining such small droplets is relevant, since the microarray of Fig. 3 was prepared with an experimental setup that was not optimized for the new printing technique. Altogether this proves the feasibility of the laser forward printing technique for depositing uniform microdroplets.

The influence on the printing process of the main process parameter, laser pulse energy, was investigated through the deposition of series of microdroplets at different energies for a fixed focusing depth of 30 µm (Fig. 4a). Nearly circular droplets, perfectly suitable for printing applications, were obtained at all the analyzed energies above 4.2 µJ. At this particular energy the deposits consist of bunches of very small droplets, with a preferential distribution along the axis of the series, and with no liquid deposition observed below 4.2 µJ. The most striking feature in the microarray of Fig. 4a is, however, the abrupt increase in droplet diameter that takes place around 5.5 µJ (this will be called the transition energy). Such abrupt change can be clearly observed in the plot of droplet diameter versus laser pulse energy of Fig. 4b. Above the transition energy, the droplet diameter presents a linear increase with energy, with a slope of about 9.2 µm/µJ; below the transition, a definitive conclusion about the specific evolution of the diameter with energy cannot be inferred with only two data points

#132085 - $15.00 USD Received 22 Jul 2010; revised 10 Sep 2010; accepted 10 Sep 2010; published 29 Sep 2010

available. However, if a linear relation were assumed, a slope of about 8.4 µm/µJ would be obtained, a value quite similar to the previous one. In contrast, in the transition the diameter suffers a dramatic increase of about 60 µm/µJ. A linear dependence of droplet diameter with laser pulse energy similar to the one encountered above the transition was previously found in LIFT experiments with no absorbing layer [28], and also with thick absorbing polymeric layers [18]. All these observations make evident the numerous resemblances between the results obtained with the new printing technique and those obtained in previous LIFT experiments, as should be expected, since the concept of LIFT is obviously the root of this new process. However, the observed differences (mainly the abrupt transition, never found in LIFT) are significant enough to question the straightforward extrapolation of the LIFT mechanisms to the new technique. In consequence, additional experiments are required to better understand the new process.

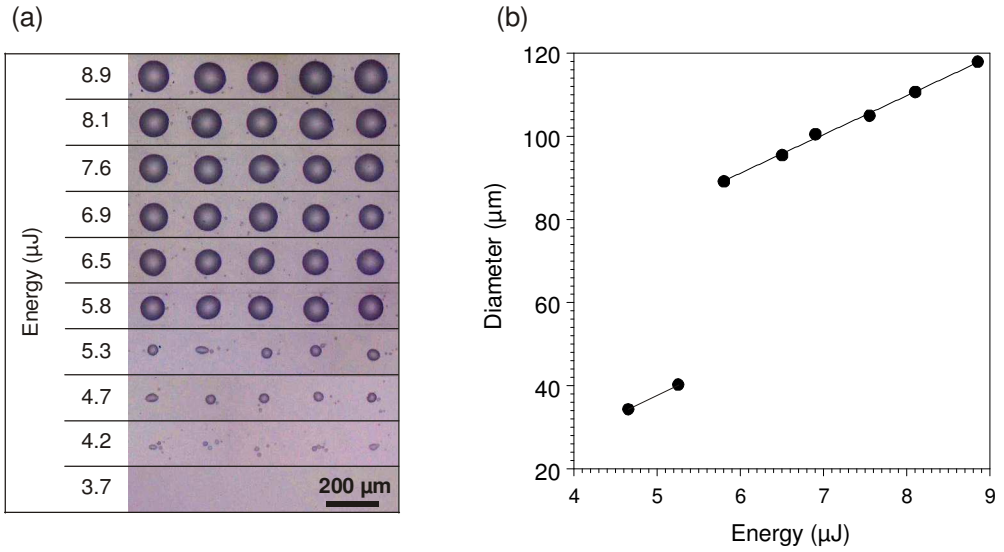

Fig. 4. a) Array of microdroplets printed with the film-free laser forward printing technique at varying laser pulse energy. The focusing depth is about 30 µm. b) Plot of the corresponding droplet diameters versus laser pulse energy.

Time-resolved imaging can help reveal the precise mechanisms responsible for material transfer during the laser forward printing of transparent and weakly absorbing liquids. With the purpose of elucidating the origin of the observed abrupt transition in the evolution of droplet diameter with laser pulse energy, series of images were acquired at two different energies, one below and one above the transition energy.

The first series of images, obtained at a laser pulse energy of about 5.0 µJ, is presented in Fig. 5a. In the analysis of the images it must be taken into account that the liquid free surface reflects quite well the incoming light; so, all the observed features are accompanied by their mirror images. Furthermore, the shadows and fringes observed in the background are due to diffractive and interferential effects generated by the use of a highly coherent illumination source. The action of the laser pulse results in the formation of a nearly hemispherical protrusion in the liquid surface. The protrusion grows fast, and at times as early as 1 µs after the laser pulse a thin needle-like jet originates from its pole. The jet develops while the protrusion collapses, and keeps on advancing with an estimated speed of about 45 m/s. Between 5 and 10 µs a second protrusion appears. The preferential growth along the axial direction of this second protrusion, with little lateral expansion, indicates that it would be better qualified as a jet. In fact, this second thick jet seems to emerge from a crater developed in the liquid surface, an issue which will be much clearer in the images obtained at a higher energy. The second jet progresses together with the first one, at an initial speed which has

#132085 - $15.00 USD Received 22 Jul 2010; revised 10 Sep 2010; accepted 10 Sep 2010; published 29 Sep 2010

been estimated to be of around 5 m/s. At about 15 μs the first jet breaks up into multiple droplets, which are projected along the vertical direction, and the second jet starts a recoiling process until it finally disappears at about 40 μs.

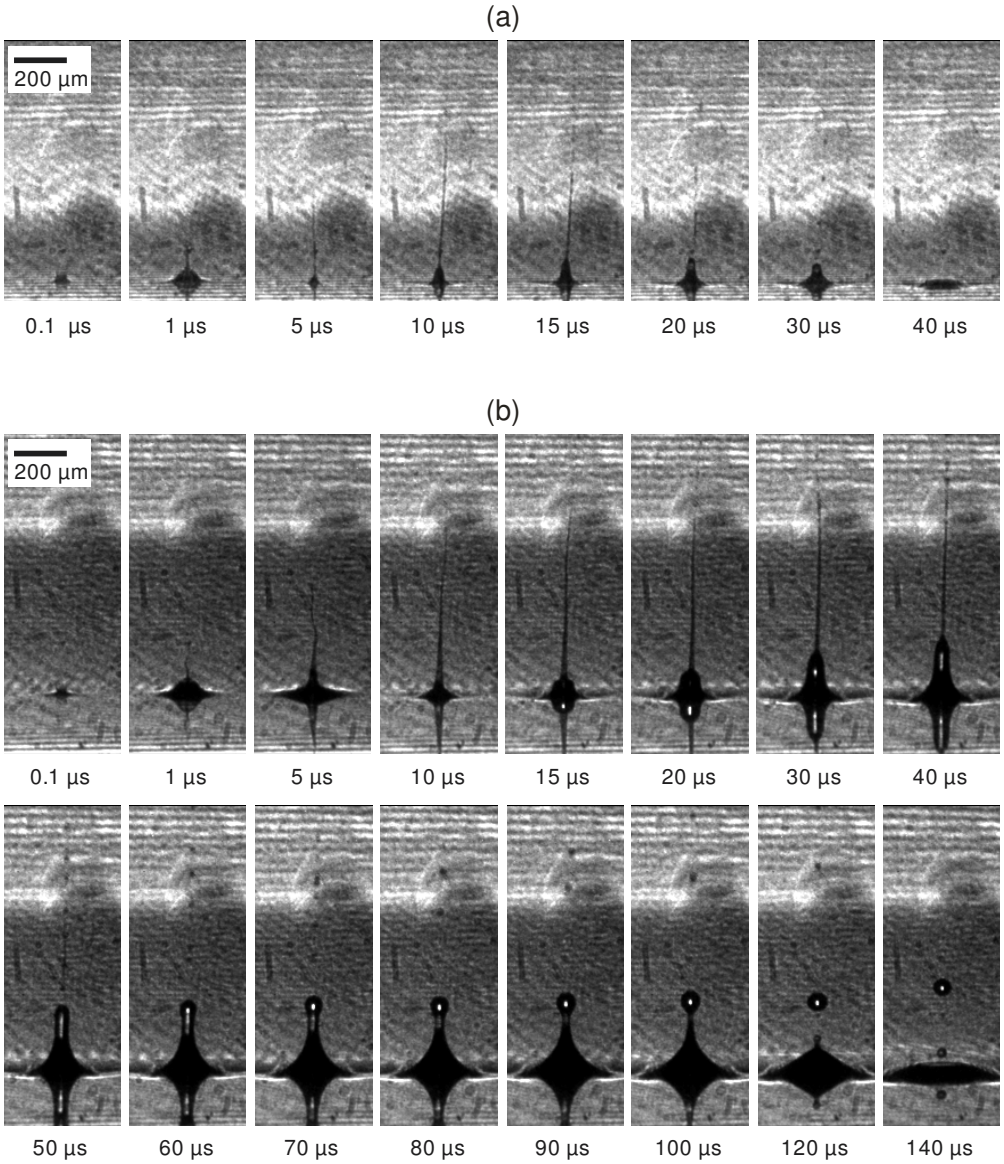

Fig. 5. Series of time-resolved images of the ejection of liquid generated with the film-free laser forward printing technique at a laser pulse energy of a) 5.0 μJ and b) 8.0 μJ. The focusing depth is about 30 μm, and the aperture time is 100 ns in all the images.

The dynamics of liquid ejection observed at a laser pulse energy of 8.0 μJ (Fig. 5b) are similar to those corresponding to 5.0 μJ for the early times. A nearly hemispherical protrusion appears in the liquid surface, from which pole a needle-like jet develops. After the collapse of the protrusion the second jet appears, following the first one in its progression. In this case both jets are thicker than those of the first series of images, and it is perfectly evident that the second one emerges from a crater that expands radially. The speed of the first jet is about 60 m/s, and although the onset of breakup is difficult to appreciate in the images, it is clear that the process starts from the jet tip and that after 50 μs this first jet completely disintegrates in a

#132085 - $15.00 USD Received 22 Jul 2010; revised 10 Sep 2010; accepted 10 Sep 2010; published 29 Sep 2010

set of very small droplets which are projected upwards. The most singular aspect of this second series of images, however, concerns the second jet. It initially advances following a very stable progression with a speed of about 6 m/s, but after 60 μs its shape starts changing, and at 70 μs the changes are really apparent: its central part progressively thins, developing a neck, while the tip becomes spherical. At 120 μs the neck pinches off, releasing a perfectly spherical droplet, about 60 μm in diameter, which flies away from the liquid free surface at a speed of around 3 m/s. At 140 μs a second pinch-off occurs, resulting in a second and smaller droplet, around 30 μm in diameter, which seems to recede and is finally reabsorbed by the liquid in the reservoir.

The results of these experiments clearly reveal that, although presenting common features, the mechanisms of liquid transfer in the new laser forward printing technique are quite more complex than those corresponding to LIFT, as the analysis of the microarray of Fig. 4a reveals.

5. Discussion

In all the described experiments, the radiation of the laser pulse was absorbed inside the transparent water solution in a small region around the beam waist through multiphoton and avalanche ionization [29]. Strong absorption in that position resulted in optical breakdown of the solution, which gave rise to the formation of a highly-excited and highly-confined plasma. This thesis is consistent with previous measurements: the intensity required to induce optical breakdown in water with 340 fs pulses of 1040 nm laser radiation has been measured to be around 3×10^{12} W/cm^2 [30]. Although both the pulse duration (450 fs) and the wavelength (1027 nm) of the laser used in the experiments here presented are not identical to the previous ones, they are similar enough, and since in all cases the laser intensity (about 10^{14} W/cm^2) is higher than the measured threshold, there can be no doubt that breakdown is taking place.

Being highly-confined, the laser-generated plasma expands rapidly, resulting in the formation of a cavitation bubble [22] close to the liquid free surface. The growing protrusion observed in the first images of Figs. 5a and 5b precisely corresponds to the expansion of that bubble, which pushes upwards the thin layer of liquid above it. The dynamics of the expansion of a bubble close to the free surface of a liquid has been previously studied [31,32]. In these works it was found that the process usually leads to the formation of needle-like jets which appear during bubble expansion, like the first jets observed in both series of images. They arise from the non-isotropic character of such expansion: the bubble displaces easily the thin liquid layer between it and the free surface, while encountering significant resistance to displacing the surrounding bulk liquid. This generates a pressure gradient between the bubble sides and its pole, which induces flow along the bubble walls and towards that pole. There the convergence of flow generates a pressure increase which is released in the form of two emerging jets, one outwards, and another one inwards (the so-called counterjet, not visible in the images of Fig. 5). The formation of this type of jets has also been observed in LIFT experiments, and described in detail [33,34]. Once fully developed, they keep on advancing while progressively thinning, until they break into multiple minuscule droplets due to the onset of Plateau-Rayleigh instabilities [34,35].

The origin of the second jets, not observed during LIFT of liquid films, is different. In contrast to the first ones, they appear during the collapse of the bubble, and emerge from the center of a crater originating in the liquid surface. It is precisely the presence of such crater which provides the main clue for interpretation. The internal pressure in the bubble decreases during expansion, and at the end of this stage the pressure is so low that it cannot counterbalance the effect of both external pressure and surface tension, which leads to its rapid collapse. This results in the fast recession of the liquid free surface surrounding the bubble below the unperturbed level, which in fact constitutes the formation of the crater. After achieving its maximum depth, the crater will collapse in turn, tending to restore the liquid free surface to the unperturbed level. However, the collapse of a depression generated in a liquid surface seems to follow an evolution quite independent of what caused it [36]: the walls of the depression collapse radially inward while its bottom accelerates upward, a process that

#132085 - $15.00 USD Received 22 Jul 2010; revised 10 Sep 2010; accepted 10 Sep 2010; published 29 Sep 2010

induces an inertial focusing of the flow towards the symmetry axis which results in the generation of a jet. Eruption of liquid jets from collapsing depressions has indeed been observed in a number of diverse instances, like during the onset of standing waves in a liquid surface [36] or during the burst of bubbles [37], though probably the most representative case is the free-fall of a drop on a liquid surface [38,39]. This last kind of jet has sometimes been called 'Worthington jet' [40] after the pioneering work on time-resolved imaging of A.M. Worthington [38], who first discovered its formation. In summary, the mechanisms leading to the formation of the two different kinds of jets appear to be completely different: while the first jets are due to the expansion of the laser-generated cavitation bubble, the second jets arise from the collapse of the crater produced after the bubble collapse.

The formation of the neck, pinch off and further droplet emission observed in the second jet is a phenomenon very characteristic of thick jets [35]. Essentially, droplet ejection is driven by a competition between inertial and surface tension forces, which allows explaining the differences observed between the images of Fig. 5a and 5b. For low laser pulse energy (5.0 μJ, Fig. 5a), few liquid is displaced to generate the second jet. This has little inertia, and recoils without emitting any droplet. Conversely, at 8.0 μJ more liquid is displaced, developing a much thicker jet with enough inertia to allow the detachment of up to two droplets from its tip, one which advances and one which seems to recoil. This difference in dynamics between the first and further droplets generated from the breakup of the jet is also characteristic of Worthington jets [41].

The series of time-resolved images (Fig. 5) also help explain the main features observed in the study of the influence of laser pulse energy on the morphology of the printed droplets (Fig. 4), and in particular the abrupt transition observed around 5.5 μJ. For laser pulse energies leading to no droplet deposition, the bubble pressure is not high enough to allow the formation of a needle-like jet; or alternatively an incipient jet can be formed, but it does not have enough energy to reach the substrate and will recoil towards the liquid in the reservoir, as has been previously observed in LIFT experiments [34]. The deposits obtained below the transition energy are due to contribution only from the first needle-like jet (the second jet recoils at a short distance from the free surface). Thus, the droplet bunches observed at 4.2 μJ are the result of a very thin jet which breaks before reaching the substrate. At higher energies the first jet is thicker and more stable, and will be able to contact the substrate before breakup, leading to the formation of a well-defined droplet, as it has been observed and described in detail under analogous conditions in LIFT experiments [42]. Following this interpretation, it cannot be excluded that the origin of the sporadic satellites found in the microarray of Fig. 3 is the partial breakup of the relatively stable needle-like jet, instead of the pinning effect previously claimed. Above the transition energy, however, there is a double contribution to the deposited droplet: on one hand, the first needle-like jet can contact the substrate and thus feeds the growing droplet, and on the other hand, the droplet emitted from the tip of the second jet, flies across the air gap and finally lands on the position where the former sessile droplet arising from the first jet was deposited. This represents an important additional contribution to the printed droplet. Such contribution would depend on the detachment of the flying droplet, a phenomenon which is activated by a small increase in the energy. This allows clarifying the origin of the abrupt transition observed in the evolution of the deposited droplet diameter versus laser pulse energy. Eventually, at much shorter gaps between the substrate and the liquid surface, a transition could also be possible, since the second jet can contact the substrate before any droplet would have been emitted from the tip. In this case, however, the transition observed in the evolution of the droplet volume would probably not be so abrupt. Finally, it has to be noted that in addition to the contribution of the emitted flying droplet to the sessile droplet, the eruption of the second jet can have another relevant consequence from a technological point of view. As it is clear from Fig. 5b, the formation of the crater results in a significant perturbation of the liquid surface, perturbation that may take a few hundreds of microseconds to relax. Taking into account the shallow focusing of the laser beam inside the liquid, this effect can be detrimental when very high repetition rates are desired. On the other hand, it must also be stated that the perturbation is clearly reduced at low laser pulse energies

#132085 - $15.00 USD Received 22 Jul 2010; revised 10 Sep 2010; accepted 10 Sep 2010; published 29 Sep 2010

(Fig. 5a), precisely the most interesting working conditions since they provide the highest degrees of resolution.

6. Conclusion

The laser-based technique developed in this work allows printing microdroplets of transparent and weakly absorbing liquids without the constraint of preparing the liquids in thin film form, and operating in a forward configuration that avoids any restriction concerning the optical properties of the substrate to be printed. The printing mechanism is mediated by the formation of liquid jets which result from the dynamics undergone by a cavitation bubble generated close to the liquid free surface through the subsurface focusing of a laser pulse. Such dynamics proceed through the ejection of a first long and thin jet during bubble expansion, and through the formation of a second shorter and thicker jet which emerges from the crater resulting from bubble collapse. At low laser pulse energies the mechanism responsible for microdroplets formation is due to the contact of the first jet with the substrate, while at high energies, droplets emitted from the second jet tip during breakup also contribute to the growth.

Acknowledgment

This work is part of a research program funded by MCI of the Spanish Government (Projects MAT2007-62357 and CSD2008-00023), and Fondo Europeo de Desarrollo Regional (FEDER).

#132085 - $15.00 USD Received 22 Jul 2010; revised 10 Sep 2010; accepted 10 Sep 2010; published 29 Sep 2010